Oligomerization of the EGF Receptor Transmembrane Domain: A ^{2}H NMR Study in Lipid Bilayers†

David H. Jones, Alan C. Rigby,‡ Kathryn R. Barber, and Chris W. M. Grant*

Department of Biochemistry, University of Western Ontario, London, Ontario, Canada, N6A 5C1

Received March 11, 1997; Revised Manuscript Received July 29, 1997⊗

ABSTRACT: During the course of a previous study by wideline ^{2}H NMR, we noted spectral features suggesting the possibility of monitoring homodimer/oligomer interactions between transmembrane domains of the EGF receptor in lipid bilayers [Rigby, A. R., Shaw, G. S., Barber, K. R., & Grant, C. W. M. (1996) *Biochemistry 35,* 12591−12601]. In the present work this possibility was explored using the 34-residue peptide $EGFR_{tm}$. The peptide sequence included the 23 amino acid hydrophobic stretch thought to span the membrane (Ile_{622}−Met_{644} of the EGF receptor), plus the first 10 amino acids of the receptor's cytoplasmic domain (Arg_{645}−Thr_{654}). Selective deuteration was carried out at sites corresponding to Ala_{623}, Met_{644}, and Val_{650}. Samples were studied from 12 to 65 °C by ^{2}H NMR in fluid membranes having low peptide concentration (1 mol %) or high peptide concentration (6 mol %). Methyl groups proved to be technically particularly attractive probe locations. Reversible homodimer/oligomer interactions were detected in membranes of the common natural phospholipid 1-palmitoyl-2-oleoylphosphatidylcholine (POPC), without cholesterol. Effects on the EGF receptor transmembrane domain included alterations in peptide backbone motional order and/or conformation at the site of Ala_{623} within the membrane, and alterations in motional properties of the Val_{650} side chain in the cytoplasmic domain. There was little spectral evidence of stable oligomer formation except at the lowest temperature studied. Addition of 33% cholesterol to these membranes was accompanied by spectral changes consistent with the formation of more stable peptide oligomers, and by evidence that peptide−peptide interactions were sensed at all three probe locations. Peptide−peptide interactions remained easily reversible, particularly at higher temperatures. Freeze−fracture electron microscopy of the NMR samples demonstrated peptide-related intramembranous particles traversing the membranes. To our knowledge, this is the first electron microscopy description of receptor tyrosine kinases or their fragments in model membranes. In the presence of cholesterol, the peptide-related particles were generally larger, more sharply demarcated, and showed a tendency to cluster. These observations relate to models of receptor lateral association as an aspect of signal transduction, and to forces that may determine protein sorting and organization in cell membranes. We suggest that the cholesterol effects reflect a general phenomenon rather than one specific to the EGF receptor.

The epidermal growth factor receptor is an important class I receptor tyrosine kinase (RTK)[1] that has been studied for insight into signalling mechanisms (Marchesi, 1986; Brandl et al., 1988; Yarden & Ullrich, 1988; Hollenberg, 1991; Fantl et al., 1993; van der Geer & Hunter, 1994). It is a 170 kDa species possessing an external glycosylated portion responsible for the earliest events in recognition; a single transmembrane domain believed to participate at a variety of levels in signal transduction; and an intracellular portion exhibiting phosphorylation sites, docking sites, and protein kinase activity. As part of a broader investigation of molecular events involved in signalling at the membrane level, we have begun to use nonperturbing nuclear probes to monitor RTK motional behavior, interactions, and conformation at selected locations. Wideline ^{2}H NMR spectroscopy lends itself particularly well to such studies since it can provide information on probe-labeled receptors dispersed as minor components in fully-hydrated multicomponent membrane assemblies, at physiological temperatures (Seelig, 1977; Davis, 1983; Smith, 1984). Thus, intermolecular factors which regulate and mediate signalling events can potentially be examined directly. An extensive underpinning now exists for application of wideline ^{2}H NMR spectroscopy to membrane proteins that were previously intractable [reviewed in Opella (1986), Opella and Stewart (1989), Smith and Peersen (1992), Cross and Opella (1994), Henry and Sykes (1994), Prosser et al. (1994), Opella et al. (1994), and Smith and Bormann (1995)].

It is widely considered that the transmembrane domains of RTKs may form meaningful homo- and heterodimer/oligomer relationships in cells [reviewed in Wofsy et al. (1992), Bormann and Engelman (1992), Fantl et al. (1993),

† This research was supported by an operating grant to C.W.M.G. from the MRC of Canada. NMR spectroscopy was carried out in the McLaughlin Macromolecular Structure Facility, established with joint grants to the department from the London Life Insurance Co., the R. S. McLaughlin Foundation, the MRC Development Program, and the Academic Development Fund of UWO.

* To whom correspondence should be addressed.

‡ Present address: Department of Biochemistry, Tufts University, New England Medical Center, 136 Harrison Ave., Boston, MA 02111.

⊗ Abstract published in *Advance ACS Abstracts,* September 15, 1997.

[1] Abbreviations: EGF, epidermal growth factor; $EGFR_{tm}$, 34 amino acid peptide corresponding to the EGF receptor transmembrane domain plus 10 residues of the cytoplasmic domain; POPC, 1-palmitoyl-2-oleoylphosphatidylcholine; TFE, trifluoroethanol; [d_4]Ala_{623}, [d_3]Met_{644}, [d_8]Val_{650}, deuterated amino acids corresponding to the indicated positions in the human EGF receptor; RTK, receptor tyrosine kinase.

S0006-2960(97)00547-3 CCC: $14.00

Hynes and Stern (1994), Lemmon and Engelman (1994), van der Geer and Hunter (1994), Heldin (1995), and Earp et al. (1995)]. Many workers have suggested such interactions to be critical early events in signal transduction pathways involving RTKs. The class I species, EGF receptor and neu/HER2, have served as platforms for the development of innovative and compelling mechanisms for such effects (Bargmann & Weinberg, 1988; Schlessinger, 1988; Brandt-Rauf et al., 1989, 1990, 1995; Sternberg & Gullick, 1989, 1990; Gullick et al., 1992; Smith et al., 1996). Nevertheless, controversy surrounds the details of the proposed mechanisms, including the role of conformation, motifs, and H-bonding. Moreover, while receptor clustering is often seen as a triggering event, some workers have submitted that in fact monomers may be active forms in the same or related pathways (e.g., Biswas et al., 1985; Northwood & Davis, 1988; Carraway & Cerione, 1993; Hazan et al., 1995; Adelsman et al., 1996; Gardina & Manson, 1996; Tatsuno et al., 1996).

The peptide $EGFR_{tm}$, corresponding to residues 621−654 of the human EGF receptor, was prepared by solid phase synthesis. The sequence included the putative transmembrane region (residues 622−644) and a 10-residue stretch of the cytoplasmic domain that included the Thr_{654} residue which is phosphorylated during EGF-mediated signal transduction (Hunter et al., 1984). A biotinylated lysine residue was substituted for the (extracellular) Ser_{621} residue to permit future studies of material selectively immobilized in bilayers. Three different deuterated amino acids were incorporated at topographically distinct sites within $EGFR_{tm}$. Methyl groups were chosen as deuteron locations because of the relatively good signal-to-noise ratio afforded by three equivalent nuclei. Perdeuterated alanine at the position corresponding to Ala_{623} of the human EGF receptor ([d_4]Ala_{623}), and methionine deuterated selectively in the methyl group at the position corresponding to Met_{644} of the human EGF receptor ([d_3]-Met_{644}), provided probes within the putative transmembrane region. A perdeuterated valine ([d_8]Val_{650}) was located six residues external to the membrane's cytoplasmic surface in the aqueous compartment, occupying the position of Val_{650} in the natural receptor sequence.

MATERIALS AND METHODS

1-Palmitoyl-2-oleoyl-3-*sn*-phosphatidylcholine (POPC) was obtained from Avanti Polar Lipids, Birmingham, AL, and was used without further purification. 9-Fluorenylmethyl *N*-succinimidylcarbonate (FMOC-OSu) and cholesterol were from Sigma, St. Louis, MO. Deuteromethyl-L-methionine ([d_3]Met), perdeuterated L-alanine ([d_4]Ala), and deuterium-depleted water (<0.5 ppm of ^2H) were from Isotec (Miamisburg, OH). Perdeuterated L-valine ([d_8]Val) was from Cambridge Isotope Laboratories (Andover, MA). FMOC-blocked amino acids were synthesized following standard procedures (Atherton & Sheppard, 1989). Product purity was checked by TLC on Merck, silica gel 60 plates against an FMOC-derivative standard. $EGFR_{tm}$ was synthesized by Chiron Mimotopes Pty. Ltd. (Clayton, Australia): the sequence was confirmed by mass spectroscopy and amino acid analysis, purity >90−95% as described elsewhere (Rigby et al., 1996).

Samples were prepared as unsonicated liposomes *via* the following general protocol. TFE (2,2,2-trifluoroethanol, 4 mL Aldrich, NMR grade, bp 77−80 °C) was added to dry peptide (up to 10 mg), and appropriate amounts of dry lipid were then weighed in and dissolved with warming to 55 °C. Samples were allowed to sit at this temperature for at least 30 min after visually-apparent complete dissolution. Solvent was rapidly removed under reduced pressure at 45 °C on a rotary evaporator to leave thin films in 50 mL round-bottom flasks. These were subsequently held for 18 h at 23 °C under high vacuum. Hydration was with 25 mM HEPES, pH 7.1, or with 30 mM HEPES with 20 mM NaCl and 5 mM EDTA, pH 7.1−7.3 (both made up in deuterium-depleted water). Samples were warmed to 35 °C without vortexing during hydration to minimize production of small vesicles.

^2H NMR spectra were acquired at 76.7 MHz on a Varian Unity 500 spectrometer using a single-tuned Doty 5 mm solenoid probe, with temperature regulation to ±0.1 °C. A quadrupolar echo sequence ("SSECHO" from the Varian pulse library) was employed with full phase cycling and a $\pi/2$ pulse length of 5−6 μs. A pulse spacing of 20−30 μs and a repetition time of 100 ms were chosen to optimize the final S/N ratio while avoiding spectral distortion and saturation after experimentation with longer and shorter values. The spectral sweep width was 100 kHz.

Samples for freeze−fracture electron microscopy were withdrawn directly from the samples prepared for ^2H NMR and thus had the same history. Prior to the "quenching" step that preserves sample structure for platinum shadowing, samples were incubated at room temperature. Frozen samples were freeze-fractured at -110 °C and shadowed in a Balzers BAF 301 apparatus equipped with electron beam guns. Replicas were cleaned initially in $NaClO_4$, rinsed with distilled water, and immersed in 1/1 acetone/ethanol for 1 h to remove residual lipid. Replicas were picked up on 400 mesh copper grids and viewed in a Phillips EM300 electron microscope.

†KI**A**TG**M**V**G**A**LL**L**LL**V**V**A**L**G**I**G**L**F****M**RR**R**H**I****V**RKRT

FIGURE 1: Sequence of the 34 amino acid peptide $EGFR_{tm}$, representing residues Ile_{622}−Thr_{654} of the human EGF receptor. The putative transmembrane domain has been underlined (cytoplasmic domain to the right). Deuterated amino acids are indicated by boldface letter symbols: perdeuterated alanine was substituted for Ala_{623} ([d_4]Ala_{623}), methionine deuterated selectively in the methyl group for Met_{644} ([d_3]Met_{644}), and perdeuterated valine for Val_{650} ([d_8]Val_{650}). A biotinylated lysine residue (†) replaced the extracellular Ser_{621}.

RESULTS

The amino acid sequence for the 34-mer, $EGFR_{tm}$, is shown in Figure 1. The suggested transmembrane portion calculated using the method of Rost and colleagues (Rost, 1996) has been underlined. Locations of amino acids with deuterated side chain CD_3 groups are indicated by boldface letters.

For molecules undergoing rapid axially symmetric rotation in membranes, the spectrum of a given deuterium nucleus is characterized by a "Pake doublet" whose splitting at the point corresponding to 90° field orientation is

$$\Delta\nu_Q = (3/8)(e^2Qq/h)S_{mol}|3\cos^2\theta_i - 1| \qquad (1)$$

where e^2Qq/h is the nuclear quadrupole coupling constant [165−170 kHz for an aliphatic C−D bond (Seelig, 1977;

Davis, 1983; Smith, 1984)], S_{mol} is the molecular order parameter (assuming axially symmetric order) describing orientational fluctuations of the molecule relative to the bilayer normal, and θ_i is the average orientation of each C−D bond relative to the molecular rotation axis. A central shift of spectral intensity is common for deuterons undergoing less smoothly continuous axial rotation ["axially asymmetric rotation" (see below: Huang et al., 1980; Meier et al., 1986; Siminovitch et al., 1988; Auger et al., 1990; Morrow et al., 1995)]. Sharper single peaks occur in the middle of spectra of samples such as those studied here, attributable to residual deuterated water and to the presence of some very small vesicles for which the quadrupole splittings are motionally averaged to zero (the latter occurs at the spectral center and the former is offset about 0.3 kHz downfield).

Equation 1 dictates that a CD_3 group on an immobilized peptide side chain should give rise to a single Pake doublet of some 40 kHz splitting (this presumes rotational motion about the C−CD_3 axis, which is always the case except at temperatures far below 0 °C). For $EGFR_{tm}$ at 6 mol % in bilayer membranes, we have demonstrated that the dominant spectral features approximate single Pake doublets for each CD_3 group (Rigby et al., 1996). Where non-methyl deuterons existed, these made insignificant contributions to the spectra due to their low relative numbers and relaxation effects (Lee et al., 1995). Thus, the spectral feature contributed by [d_4]Ala_{623} was one Pake doublet, while [d_8]Val_{650} gave a pair of doublets (one for each valine methyl group). [d_3]Met_{644} produced a doublet with evidence of motional asymmetry manifest as broad, peaked spectral intensity buildup in the middle of the doublet. All spectral widths were less than 40 kHz, yet spectra were essentially Pake doublet in nature at physiological temperatures; hence, it is clear that deuterated $EGFR_{tm}$ undergoes rapid axial rotation in these membranes.

Figure 2 displays wideline spectra typical of those which initially suggested to us the possibility that $EGFR_{tm}$ homodimer/oligomer interactions in liposomes could be monitored by ^2H NMR. These spectra represent membranes containing peptide deuterated simultaneously on the three amino acids indicated in Figure 1. Samples were well above the POPC fluid/gel phase transition temperature of −3 °C (Davis & Keough, 1995) and in a range in which POPC/cholesterol mixtures are fluid and homogeneous (Thewalt & Bloom, 1992). Sharpening of Pake features in Figure 2 occurred as a result of either raising the temperature (compare a given concentration at 12 °C to the same concentration at 45 °C) or lowering the peptide concentration (compare 6 mol % to 1 mol % at a given temperature). Such effects might be explained as arising from alterations in probe motion and/or orientation, associated with peptide−peptide interaction. For all samples, including the more selectively deuterated ones described below, there was a continuous increase in spectral width as temperature was lowered—as anticipated due to the greater motional order at low temperature (S_{mol} term in eq 1).

Detailed interpretation of spectra such as those in Figure 2 was complicated by overlap of peaks arising from the multiple probe locations. Figures 3−5 present typical results of experiments designed to explore the effects of peptide concentration in samples containing $EGFR_{tm}$ with only one deuterated amino acid at a time. Spectra are grouped in vertical pairs: the higher peptide concentration above the identical sample with low peptide concentration. Features of spectra for $EGFR_{tm}$ deuterated at Ala_{623} (Figure 3) should reflect the least motional complexity since the CD_3 group of alanine is attached directly to the peptide backbone (no independent side chain freedom of motion). In POPC membranes without cholesterol, a Pake doublet was obtained at 65 °C (Figure 3, top left pair). Note also the very sharp central peaks, which reflect the water peak referred to above and traces of a transmitter spike. As temperature decreased, the Pake doublet spectral shape became progressively obscured by broad central intensity shift, with eventual complete loss of identifiable Pake features at the lowest temperature studied (12 °C, bottom left). At the higher peptide concentration, spectral intensity decreased by 47% at 12 °C, apparently associated with peptide immobilization in spite of the fact that the host matrix is fluid above −3 °C (Davis & Keough, 1985). For the comparable sample with 1 mol % peptide in the membrane, only 5% intensity loss occurred, which is not significant. Quadrupole splittings measured at the 90° spectral edges are listed in Table 1: for spectra in which Pake features had been lost (12 °C), half-height width is recorded. Of the intermediate temperature spectra run, only that corresponding to 25 °C is displayed (Figure 3) since this represented a point at which spectral shape began to show a marked tendency to broad central intensity buildup as temperature was reduced. Note that at 25 °C and above, the peptide in POPC alone demonstrated obvious reduction in spectral splittings (by some 25%) in going from 6% to 1% peptide. Interestingly, upon addition of cholesterol to such samples, the effect of peptide concentration on splitting was not significant for the Pake spectra (Figure 3, right-hand column, 65 and 35 °C). However, temperature reduction had a greater effect on line shape. Thus, the 35 °C intermediate temperature is shown in this case since it is the point at which spectra began to

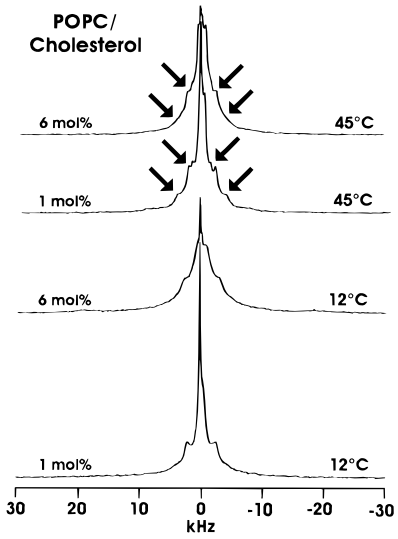

FIGURE 2: ^2H NMR spectra corresponding to $EGFR_{tm}$ in which all three deuterated amino acids coexist. In each case, the peptide has been incorporated into bilayers of POPC containing 33 mol % cholesterol. Data are presented as vertically-paired spectra to permit comparison between membranes having 6 mol % peptide *vs* 1 mol % peptide in the membrane. Paired spectra are included for samples at 45 °C (upper pair) and 12 °C (lower pair). Arrows in the upper spectral pair indicate Pake features to be examined as a function of peptide concentration. Each spectrum represents 150 000 accumulated transients for the samples containing 6 mol % peptide and 565 000−612 400 transients for the 1 mol % samples.

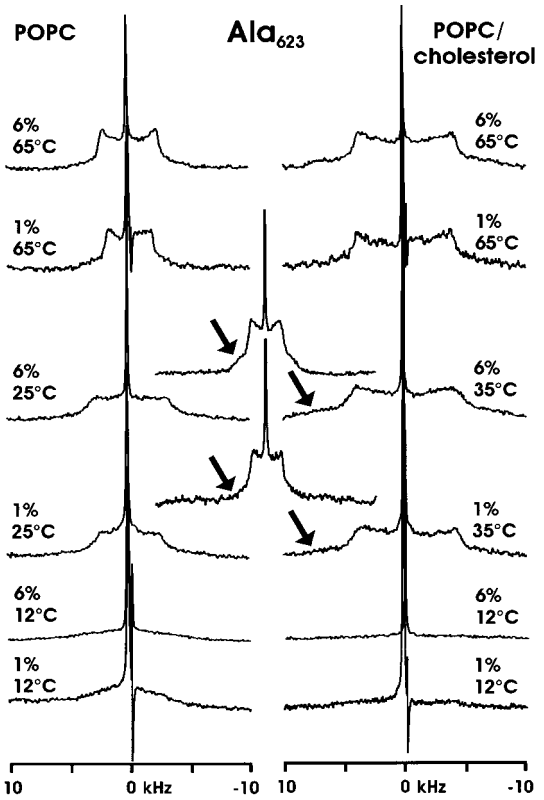

FIGURE 3: ^{2}H NMR spectra corresponding to $EGFR_{tm}$ having the single deuterated amino acid [d_4]Ala_{623}. Peptide was incorporated at high and low concentrations into bilayers of POPC (left-hand column) or POPC/cholesterol (right-hand column). Data are presented as vertically-paired spectra to permit comparison between membranes having 6 mol % peptide *vs* 1 mol % peptide. Temperature extremes of 65 and 12 °C are illustrated in each case. The intermediate temperature point 25 °C is shown for POPC membranes, and 35 °C for POPC/cholesterol membranes since these were points at which the spectral shape began to clearly lose its Pake nature with temperature reduction. The 35 °C (POPC/cholesterol) intermediate spectra have also been shown on an expanded frequency axis of 60 kHz (central column insert) to better demonstrate the line shape changes for this pair: a shoulder suggestive of asymmetric motion occurs at the higher peptide concentration (arrows indicate corresponding frequencies in each spectrum). Spectra represent 200 000−500 000 accumulated transients. Temperature effects on spectral intensity were measured on a given sample without changing its location in the probe. Very sharp central peaks reflect the water peak referred to in the text and traces of a transmitter spike.

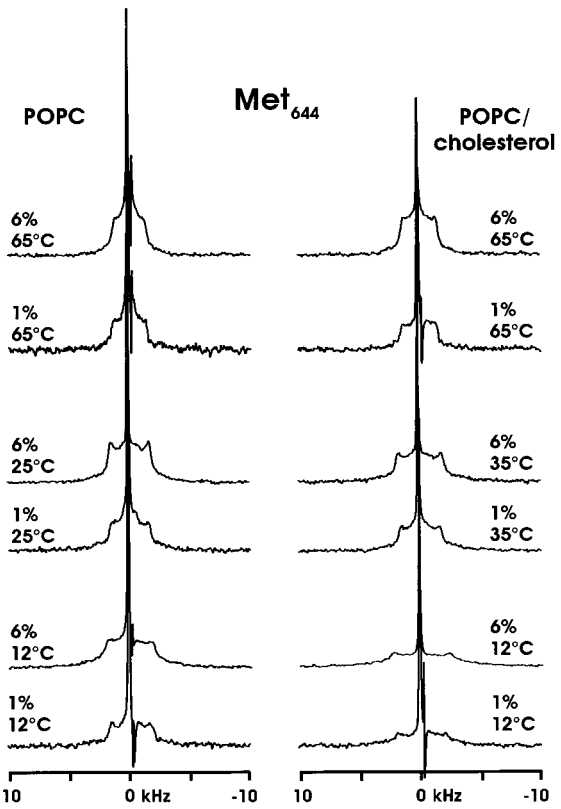

FIGURE 4: ^{2}H NMR spectra corresponding to $EGFR_{tm}$ having the single deuterated amino acid [d_3]Met_{644}. Peptide was incorporated at high and low concentrations into bilayers of POPC (left-hand column) or POPC/cholesterol (right-hand column). Data are presented as vertically-paired spectra to permit comparison between membranes having 6 mol % peptide *vs* 1 mol % peptide. Temperature extremes of 65 and 12 °C are illustrated in each case. The intermediate temperature point 25 °C is shown for POPC membranes, and 35 °C for POPC/cholesterol membranes since these were points at which the spectral shape began to clearly lose its Pake nature with temperature reduction. Spectra represent 200 000−500 000 accumulated transients. Temperature effects on spectral intensity were measured on a given sample without changing its location in the probe.

demonstrate asymmetric-motion-related obscuration of the Pake doublet by central intensity buildup. Although a clear Pake doublet was once again obtained at 65 °C, this became quickly distorted and characteristic of slowed peptide axial rotation as temperature was reduced for the 6 mol % samples containing cholesterol. There was almost complete (83%) loss of spectral intensity at 12 °C in the presence of cholesterol: only the sharp artifact peaks remain as obvious features at this temperature (Figure 3, bottom right). For the 1 mol % sample containing cholesterol, peptide motional response to temperature change was less marked. This can be seen in the intermediate-temperature spectrum at 35 °C in which only the 6% sample shows striking distortion of the Pake shape (better demonstrated in the insert spectra which are displayed on expanded frequency axes; arrows mark comparable frequencies). Similarly, the 1% sample displayed only 49% intensity loss at 12 °C.

Spectra to be compared for intensity changes were run on the same sample, without manipulation in the probe. Killian et al. (1996) have cautioned that irreversible aggregation of some hydrophobic peptides can occur in TFE (and hexafluoroisopropyl alcohol). This did not appear to be a significant problem with $EGFR_{tm}$: there was no hysteresis in the spectra obtained, and spectral features of samples containing 6 mol % peptide became identical to those of freshly prepared 1 mol % samples simply by adding more lipid.

Related experiments were performed for $EGFR_{tm}$ having deuterium nuclei only in the side chain methyl of the residue corresponding to Met_{644} of the natural EGF receptor (Figure 4), or only in the residue corresponding to Val_{650} (Figure 5). Probes on Met_{644} in membranes of POPC without cholesterol demonstrated no change in the overall line shape or intensity with decreasing temperature. Moreover, reducing the peptide concentration to 1 mol % did not significantly alter the quadrupole splitting or line shape. However, the sample with added cholesterol displayed a spectral intensity decrease of 33% in dropping from 65 to 12 °C for the 6 mol % peptide concentration, while no significant intensity loss was recorded for the same sample at low mole percent peptide. Similarly, peptide in the cholesterol-containing membranes showed significant differences in spectral split-

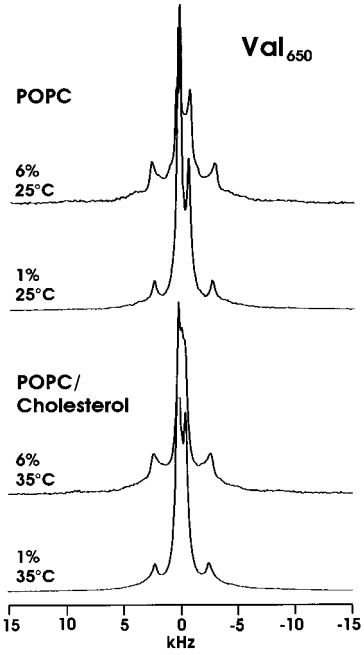

FIGURE 5: ^{2}H NMR spectra corresponding to $EGFR_{tm}$ having the single deuterated amino acid [d_8]Val_{650}. Data are presented as vertically-paired spectra to permit comparison between membranes having 6 mol % peptide *vs* 1 mol % peptide. Peptide was incorporated at high and low concentrations into bilayers of POPC (upper pair) or POPC/cholesterol (lower pair). Note that at low peptide concentration there is increased intensity buildup of the inner doublet relative to the outer doublet, as a reflection of altered side chain dynamics. Only one temperature point is shown for each type of membrane (25 °C for POPC, 35 °C for POPC/cholesterol) since [d_8]Val_{650} displayed little line shape sensitivity to temperature. Each spectrum represents 200 000−500 000 accumulated transients.

ting between the 6% and 1% samples at 12 °C (Figure 4 and Table 1).

Like methionine, the deuterated side chain of Val_{650} has potential for more complex motions. However, it is distinct from both Ala_{623} and Met_{644} in that it is geographically removed from the membrane hydrophobic domain. Spectra for Val_{650} samples in POPC alone and in POPC/cholesterol demonstrated very little line shape sensitivity to temperature. However, reduction in peptide concentration induced a marked effect on line shape in both cases: at low peptide concentrations, there was a notable tendency to increased relative intensity of the inner doublet as a reflection of greater anisotropy of side chain motion (Figure 5). Thus, spectra of the 6 mol % samples demonstrate a 1:1 intensity ratio for the inner and outer Pake doublets (confirmed by spectral depaking; data not shown here), while this ratio was some 5:1 or more (inner/outer) for the 1 mol % samples. The same changes in peptide concentration had little effect on quadrupole splitting (Table 1).

Figure 6 presents freeze−fracture electron micrographs of the structures found in the samples used for ^{2}H NMR spectroscopy. In this technique, a rapidly-frozen sample is fractured in vacuum at −110 °C, and the fracture face is immediately shadowed with an atomic layer of platinum and carbon. The fracture plane is known to split bilayer membranes between their component monolayers. The micrographs clearly demonstrate that the systems used were liposomal. Nonliposomal or amorphous structures were not seen. Clearly also, the hydrophobic membrane interior exposed by the fracture plane shows classic bilayer appearance and the presence of particulate discontinuities ('bumps'). The latter are strikingly similar to the "intramembranous particles" that characterize fracture faces of cell membranes (Pinto da Silva, 1987) and model membranes containing transmembrane glycoproteins (Grant, 1986). The particle size distribution (measured on the basis that a "particle" is a bump without visible internal fine structure, i.e., which cannot be further subdivided visually) ranged from 4.6 to 6.9 nm in the absence of cholesterol, and from 4.6 to 9.2 nm in the cholesterol-containing membranes. Note that the particles seen in the liposomes containing cholesterol also appeared more sharply resolved, and that they tended to occur in clusters.

Table 1: ^{2}H NMR Spectral Splittings ($\Delta\nu_Q$) Corresponding to Deuterated $-CD_3$ Groups in $EGFR_{tm}$[a]

deuterated amino acid	lipid	peptide concn (%)	spectral splittings ($\Delta\nu_Q$) ±0.2−0.5 kHz at temp (°C) 12	25	35	45	55	65
[d_4]Ala_{623}	POPC	6	*b*	6.4	6.0	5.6	5.1	4.7
		1	*b*	5.2	–	–	–	3.8
[d_4]Ala_{623}	POPC/chol	6	*b*	9.4	8.8	8.9	–	8.3
		1	*b*	–	8.3	–	–	8.2
[d_3]Met_{644}	POPC	6	3.9	3.4	3.1	2.9	2.8	2.5
		1	3.5	3.2	–	–	–	2.8
[d_3]Met_{644}	POPC/chol	6	5.0	4.3	3.8	3.6	–	2.9
		1	4.2	–	3.4	–	–	2.9
[d_8]Val_{650}	POPC	6	–	1.3	1.2	1.2	1.1	1.1
inner splitting		1	–	1.2	–	–	–	–
	POPC/chol	6	1.0	0.8	0.7	0.7	–	0.7
		1	–	–	0.8	–	–	–
[d_8]Val_{650}	POPC	6	–	5.8	5.4	5.2	4.9	4.7
outer splitting		1	–	5.3	–	–	–	–
	POPC/chol	6	6.1	5.6	5.2	4.9	–	4.4
		1	–	–	5.0	–	–	–

[a] In each case, peptide was assembled into bilayers of POPC, or POPC containing 33 mol % cholesterol. All samples were prepared by hydration of films dried down from TFE solution, studied as a function of decreasing temperature. The quoted estimated uncertainty reflects typical maximum variability found for samples prepared on different occasions and inter-observer variability. [b] At 12 °C, spectra of [d_4]Ala_{623} samples had become sufficiently characteristic of axially asymmetric motion that 90° edges were not readily identifiable, and there was some intensity loss. Peak widths at half-height were 10 and 6.9 kHz for the 6% and 1% samples, respectively, in POPC alone at 12 °C; and 16 and 11.2 kHz for the 6% and 1% samples, respectively, in POPC/cholesterol at 12 °C.

DISCUSSION

We have previously described ^{2}H NMR spectra of $EGFR_{tm}$ at relatively high concentration in bilayer membranes as part of a study aimed at measuring its behavior and conformational sensitivity (Rigby et al., 1996). In the present work, we sought evidence of side-to-side interactions among isolated transmembrane domains of the EGF receptor as a class I receptor tyrosine kinase, and insight into the consequences. The experiments relate to models of receptor lateral association as an aspect of signal transduction. They also relate to forces that might determine protein sorting and organization in cell membranes.

Peptide concentrations within the bilayer were chosen based on the need for an adequate number of deuterated molecules to permit NMR signal detection (1 mol % peptide being the lower limit that was readily observable), and the desire to avoid bilayer disruption by excessive peptide (6 mol % being acceptable based on the spectral results and

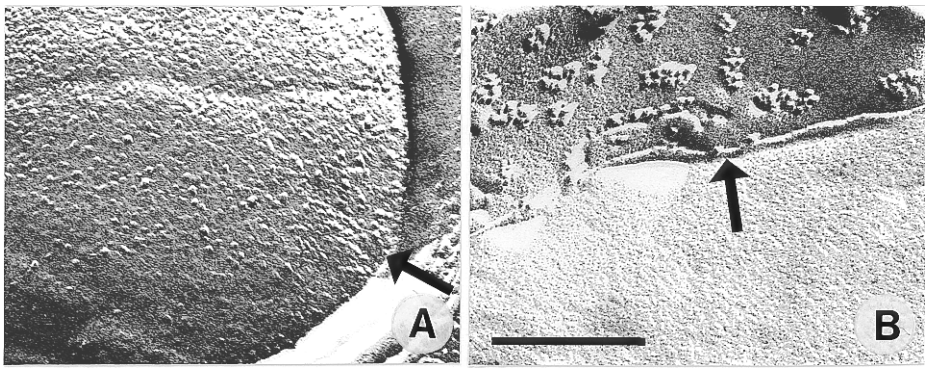

FIGURE 6: Freeze−fracture electron micrographs of typical NMR samples. Samples contained 6 mol % $EGFR_{tm}$, in POPC (A) and POPC/cholesterol (B). Arrows point from ice to liposome edge. Bar indicates 200 nm. Shadow direction is from bottom to top of page. In each case, samples were removed from NMR sample tubes of similar history, quenched from 22 °C at the same time, and fractured and shadowed together to ensure identical treatment.

electron microscopy observations described here). It is generally considered that the transmembrane portions of proteins adopt α-helical geometry (Gullick et al., 1992; Li & Deber, 1993; Lemmon & Engelman, 1994; Smith et al., 1996) [although deviation from this geometry has been indicated near the amino terminus of the EGFR transmembrane domain based on molecular modeling (Brandt-Rauf et al., 1994)]. Our previous high-resolution NMR work has shown $EGFR_{tm}$ to be α-helical between Met_{626} and Arg_{647} in the lipomimetic solvent TFE (Rigby et al., 1996, and unpublished observations), and this was the solvent used in preparing the dry lipid/peptide films that were subsequently hydrated to produce wideline NMR samples. Making the approximation that the diameter of a monomeric transmembrane α-helix is comparable to the diameter of a phospholipid molecule, one may estimate that the nearest-neighbor annulus of lipid should be at least some 12 molecules in a hexagonal membrane lattice. At 6 mol % peptide, there are 16 or 17 phospholipid molecules per molecule of peptide; i.e., 2−3 phospholipid molecules would separate maximally dispersed peptide monomers. Clearly, there is a high statistical likelihood of peptide−peptide encounters in such a system. Pursuing this simplistic approximation of a hexagonal lattice, the second lipid annulus of each monomer would be 24 molecules, and the third annulus 36. Hence, at 99 lipids per peptide (1 mol % peptide), the number of lipid molecules separating maximally dispersed peptide monomers would increase to 7−8, and peptide−peptide encounters would be significantly reduced in frequency. While even 1 mol % might be viewed as a high concentration, it has been estimated that for cell membranes in general, protein concentrations are also high, such that the probability of dimer/oligomer formation is 10^6-fold greater than that of protein existence as monomers (Grasberger et al., 1986).

CD_3 groups attached to rigid, fully immobilized macromolecules produce powder spectra characterized by a splitting of 40 kHz. The fact that spectra of $EGFR_{tm}$ observed here were narrower than 40 kHz, and yet typically Pake doublet in nature, indicates rapid axially symmetric rotation of the peptide. Following the rough calculations described above and considering that side-to-side dimer-/oligomerization would likely give rise to slower axial diffusion and/or nonaxially symmetric rotation, it is perhaps surprising that spectra of $EGFR_{tm}$ at 6 mol % are as characteristic of axially symmetric motion as they are. The implication would seem to be that for the EGF receptor transmembrane domain there is a low intrinsic tendency toward self-association. In keeping with this, Lemmon and Engelman (1994) note that there have been no reports of dimerization of the EGF receptor transmembrane domain. It is tempting to suggest that a low tendency to self-association for $EGFR_{tm}$ is consistent with the fact that EGF-induced stimulation of cells is generally considered to show unremarkable sensitivity to site-specific mutation within the transmembrane domain (Lemmon & Engelman, 1994).

Hydrophobic peptide α-helices are seen as relatively rigid structures within membranes, and are considered to pirouette about axes perpendicular to the plane of the membrane. Wobble of the helix about this axis (i.e., time-dependent variation of the angle between the helix long axis and the axis of rotation) would show up as reduction in the order parameter term, S_{mol}, in eq 1. S_{mol} has a maximum possible value of 1.0 and a minimum of 0. Superimposed on this "rigid body" motion of the helix as a whole, any local freedom of motion of the deuterium probe will tend to show up as an additional reduction in S_{mol}. Independent motion of a CD_3 group by virtue of being located on a flexible side chain or near an unraveling end of the helix would fall in this category. Side-to-side interaction with other RTK transmembrane domains in a highly fluid POPC membrane would have the potential to decrease rigid-body wobble of $EGFR_{tm}$. Clearly, peptide−peptide interactions could also affect amino acid side chain independent motions. Equation 1 dictates that any change which reduces disorder in probe motion will increase spectral splitting, and *vice-versa*. In addition, peptide−peptide side-to-side interactions might induce conformational or orientational changes in $EGFR_{tm}$ or in its amino acid side chains: such changes would affect θ_i, the second determinant of spectral splitting in eq 1.

Motional *nature* can have very important effects on spectral shape and intensity. Thus, asymmetric motion can cause a central shift in intensity for Pake doublet spectra arising from systems such as those described here. The term axially asymmetric refers to axial rotation which is less smoothly continuous: e.g., 2-fold jumps and 3(or higher)-fold jumps with unequal population weighting of available states (Huang et al., 1980; Opella, 1986; Beshah & Griffin, 1989; Auger et al., 1990; Lee & Cross, 1994). In the present ^2H NMR context, this might be expected to result if peptide aggregation occurs leading to irregular cross-sectional shape and/or restricted axial rotation. Shift of spectral shape from Pake doublet to centrally-peaked (asymmetric motion) has been recorded by Mueller et al. (1986) for deuterated tyrosine in a hydrophobic dipeptide in dipalmitoylphosphatidylcholine

bilayers upon restriction of the peptide rotational diffusion rate. MacDonald and Seelig (1988) have seen similar effects in spectra of deuterated gramicidin in fluid bilayers upon increasing the peptide concentration within the membrane. Moreover, alterations in the *rate* of motion can lead to loss of spectral intensity—for instance, if a deuterated molecule rotating rapidly within the membrane slows to the NMR time scale (10^{-4} s here). This phenomenon has been recorded for deuterated lipids whose rigid-body rotational diffusion rate slows to $10^{-4}-10^{-5}$ s (Haberkorn et al., 1977; Oldfield et al., 1978; Meier et al., 1986; Renou et al., 1989; Hamilton et al., 1994).

In the present work, we examined spectral quadrupole splitting, line shape, and intensity, as influenced by peptide concentration within fluid membranes at a given temperature. For each probe location, it was clear that $EGFR_{tm}$ was undergoing significant side-to-side interpeptide interactions. Results with the alanine probe (CD_3 group attached directly to the peptide backbone) are most readily interpretable in terms of the phenomena being addressed. $EGFR_{tm}$ deuterated at Ala_{623}, and dispersed in POPC bilayers without cholesterol, displayed significantly greater quadrupole splitting at higher peptide concentration. This could logically arise from reduction in peptide rigid-body wobble as described above. It could also arise from peptide backbone conformational stabilization. This is an exciting possibility. For instance, Ala_{623} is at a site which Brandt-Rauf et al. (1994) have considered less prone to stable helical geometry, with implications for signal transduction. However, Ala_{623} is also the third residue in the sequence of $EGFR_{tm}$, and it is known that there can be a tendency to unraveling of the ends of helical peptides (Smith et al., 1994). There was a 47% reduction in spectral intensity at 12 °C for the samples with high peptide concentration in POPC, while when the peptide concentration in the membrane was reduced to 1 mol % the intensity loss was negligible. The latter effect points to significant peptide dimer-/oligomerization with resultant slowing of axial rotation. The line shape remained relatively unaffected by temperature reduction in POPC until the lowest temperature studied (12 °C), at which point the spectrum became very distorted by central intensity buildup arising from motional asymmetry. In contrast, with the addition of cholesterol to the membranes, peptide concentration altered line shape more strikingly than it altered splitting (Figure 3 and Table 1). With cholesterol present, even at the intermediate temperature of 35 °C the high peptide concentration samples displayed deviation from Pake nature, which was not seen at low mole percent peptide. Moreover, for the high peptide concentration, there was a more striking reduction in intensity at 12 °C (83%) than had been the case without cholesterol, and even when the peptide concentration in the membrane was reduced to 1 mol %, the intensity loss was still significant (49%, i.e., close to the value seen at high peptide concentrations in membranes without cholesterol). Thus, there was also clear evidence of oligomerization-induced slowing of peptide axial rotation in cholesterol-containing membranes, and the degree of restriction of rotation was considerably greater than in POPC alone. We demonstrated previously that addition of cholesterol to POPC membranes containing $EGFR_{tm}$ dramatically increased the spectral splitting of deuterated Ala_{623} relative to Met_{644} or Val_{650} (Rigby et al., 1996). Thus, we suggest that both peptide−peptide side-to-side interactions and cholesterol addition to a fluid host matrix stabilize the peptide NH_2-terminus, resulting in a larger quadrupole splitting. This would explain why in the cholesterol-containing membranes Ala_{623} spectral splitting is not so sensitive to peptide concentration: it is already stabilized by the presence of cholesterol. But at 6 mol % peptide in the membranes containing cholesterol, dimers/oligomers can form that reduce the rate of peptide axial rotation. Since axial rotation of the entire peptide is the major contributor to line shape for the CD_3 group on alanine, its motion became slow on the NMR time scale, resulting in intensity loss and a spectrum characteristic of asymmetric axial rotation at low temperature.

Met_{644} was located in what should be a very stable α-helical stretch of the peptide hydrophobic domain. However, its CD_3 group is at the end of a flexible side chain. This seems likely to explain why it demonstrated relatively little spectral change as a function of peptide concentration [going from 6 to 1 mol % peptide induced a significant decrease in spectral width only at the lowest temperature studied (12 °C), and even then only in the presence of cholesterol]. Also there was significant loss of spectral intensity at 12 °C only for the 6 mol % peptide sample having cholesterol in the membrane—the combination of high peptide concentration, low temperature, and presence of cholesterol predisposing maximally to peptide self-association.

The Val_{650} residue, located six residues into the cytoplasmic domain and with a flexible side chain, might well be expected to be differently affected by peptide−peptide associations. The overall motional properties of the valine CD_3 groups changed in going to low peptide concentration, while spectral splittings (orientation) were little altered. The change was the same in the presence and absence of cholesterol (spectral intensity shift from the outer to the inner doublet). Given the complex motions attributable to such a side chain (Beshah & Griffin, 1989; Lee & Cross, 1994), it is not possible to assign a specific basis for this effect, which could arise from a change in rotamer populations at various levels. But it is interesting that this presents an example of peptide self-association being manifest locally only as motional changes.

Freeze−fracture preparations of the $EGFR_{tm}$ samples demonstrated that they were homogeneous and liposomal in nature even at the highest peptide concentrations studied. The presence of intramembranous particles 5−9 nm (50−90 Å) in diameter was noted in the hydrophobic interior. The association of such particles with integral membrane proteins has been well documented in both cells (Pinto da Silva, 1987) and model membranes (Grant, 1986), although it is not known precisely what a "single" particle represents. Intramembranous particle association with isolated transmembrane domains has been less well investigated. However, Segrest et al. (1974) demonstrated that a proteolytic peptide fragment containing the transmembrane domain of the glycoprotein, glycophorin, gave rise to intramembranous particles in lipid bilayers. Yamanaka and Deamer (1976) found intramembranous particles in fracture faces of lobster muscle cell membranes following extensive proteolysis of the extramembranous domains. Thus, it would appear that the sample preparation technique used in the present work is capable of incorporating transmembrane domains of RTKs in a natural spatial arrangement relative to the membrane. It is important to keep in mind that the platinum/carbon shadow

thickness of freeze−fracture EM is in the range of 2 nm. Moreover, local distribution changes can occur during the rapid freezing process. Hence, one must not read too much into subtleties of particle size and appearance. However, samples with and without cholesterol were handled identically and fractured and shadowed simultaneously, so that differences in relative particle size and distribution likely reflect genuine differences in underlying intermolecular effects. For a host matrix of POPC without cholesterol, the distribution of particles was homogeneous. In the presence of cholesterol, the particles were more sharply resolved and ranged from the same minimum size (about 5 nm) to a slightly larger maximum size (9 vs 7 nm). More strikingly, the peptide-related particles were clustered in cholesterol-containing membranes. The EM results are highly consistent with the concept that greater and/or more stable oligomerization occurs in membranes containing cholesterol.

Cholesterol is generally seen as leaving rotational diffusion rates of lipids largely unaffected in fluid membranes, while greatly decreasing their acyl chain flexibility and increasing membrane thickness (Oldfield & Chapman, 1972; Demel & de Kruijff, 1976; Yeagle, 1985; Needham et al., 1988; Keough et al., 1989; Weisz et al., 1992; Bloom, 1992; Davis, 1993; McMullen & McElhaney, 1995). Mühlebach and Cherry (1982) have postulated a role for cholesterol in regulating associations between integral membrane proteins based on their work with erythrocyte membranes treated to remove cytoskeletal attachments. They suggest that it predisposes to protein aggregation, a conclusion which seems directly relevant to the present observations. Our proposal that oligomerization increases with temperature reduction may also be reflected in cellular phenomena: Jans et al. (1989) noted greatly decreased vasopressin receptor mobility in membranes (not attributable to a membrane phase transition) below physiological temperatures. Siminovitch et al. (1988) have indicated that cholesterol can reduce lateral diffusion rates of lipids in fluid bilayers. Such a phenomenon, connected perhaps with overall reduced lipid thermal motions, could logically predispose to peptide oligomerization in the presence of significant interpeptide attractive forces. An additional consideration is that peptide oligomerization could be driven by a tendency to be excluded (phase separated) from the surrounding bilayer matrix (Grant & McConnell, 1974; Owicki et al., 1978). Strong exclusionary forces involving cholesterol would seem reasonable candidates for some aspects of membrane protein sorting mechanisms at the level of the golgi membrane [reviewed in Lemmon and Engelman (1994)].

A final consideration relevant to cholesterol effects on peptide−peptide interactions is the question of bilayer hydrophobic thickness. Presuming a right-handed α-helix of 3.6 residues per turn, the calculated length for the putative hydrophobic domain displayed in Figure 1 is 34.5 Å (Ramachandran & Sasisekharan, 1968). This compares with a calculated hydrophobic membrane thickness for POPC bilayers of 25.8 Å at 25° (*vs* 29.9 Å for the same membranes with 30 mol % cholesterol added) (Nezil & Bloom, 1992). The relevant peptide hydrophobic length would be reduced to 31.3 Å if peptide α-helices were oriented at 25° to the bilayer normal (for instance, if dimers were formed having a crossing angle of 50°). In either case, one might conclude that a greater $EGFR_{tm}$ hydrophobic mismatch occurs in the case of membranes without cholesterol, and that this mismatch will increase at higher temperatures; however, calculations of this sort are presumed to be only one aspect of protein arrangement in membranes (Mouritsen & Bloom, 1993).

CONCLUSIONS

The transmembrane domain of the EGF receptor displays a low tendency to formation of homodimers/oligomers in fluid phospholipid membranes without cholesterol at physiological temperatures. However, peptide−peptide interactions were detected at 6 mol % peptide *via* their effects on backbone motion and perhaps conformation, and *via* their effects on side chain dynamics. In this regard, it may be desirable to focus greater attention on the dynamic aspects of signalling elements, as recently indicated by Rigby et al. (1996) and by Garnier et al. (1996). The stabilizing effect of peptide−peptide association bore similarity to the ordering effect of cholesterol in fluid membranes. The tendency to stable homodimer/oligomer association of the hydrophobic domain is significantly increased by the presence of cholesterol and by reduction in temperature, while remaining reversible. Deuterium probe nuclei on methyl groups closely associated with the peptide backbone have good potential for interpretation in terms of signalling events, making alanine residues a site of choice for study. With greater understanding of the processes involved, CD_3 groups on mobile side chains such as methionine and valine can provide insight regarding local dynamics and lipid environment. Non-methyl deuterons suffer from severe difficulties of signal detection. The thin film approach to preparation of model membranes containing RTK transmembrane domains appears validated by both spectroscopy and electron microscopy, at least in the case of the EGF receptor.

REFERENCES

Adelsman, M. A., Huntley, B. K., & Maihle, N. J. (1996) *J. Virol. 70,* 2533−2544.

Atherton, E., & Sheppard, R. C. (1989) in *Solid phase peptide synthesis: a practical approach,* p 50, Oxford University Press, New York.

Auger, M., Carrier, D., Smith, I. C. P., & Jarrell, H. C. (1990) *J. Am. Chem. Soc. 112,* 1373−1381.

Bargmann, C. I., & Weinberg, R. A. (1988) *EMBO J. 7,* 2043−2052.

Beshah, K., & Griffin, R. G. (1989) *J. Magn. Reson. 84,* 268−274.

Biswas, R., Basu, M., Sen-Majumdar, A., & Das, M. (1985) *Biochemistry 24,* 3795−3802.

Bloom, M. (1992) *Physics Canada 48,* 7−16.

Bormann, B. J., & Engelman, D. M. (1992) *Annu. Rev. Biophys. Biomol. Struct. 21,* 223−242.

Brandl, C. J., Deber, R. B., Hsu, L. C., Wooley, G. A., Young, X. K., & Deber, C. M. (1988) *Biopolymers 27,* 1171−1182.

Brandt-Rauf, P. W., Pincus, M. R., & Chen, J. M. (1989) *J. Protein Chem. 8,* 749−756.

Brandt-Rauf, P. W., Monaco, R., & Pincus, M. R. (1994) *J. Protein Chem. 13,* 227−231.

Brandt-Rauf, P. W., Pincus, M. R., & Monaco, R. (1995) *J. Protein Chem. 14,* 33−40.

Carraway, K. L., & Cerione, R. A. (1993) *J. Biol. Chem. 268,* 23860−23867.

Cross, T. A., & Opella, S. J. (1994) *Curr. Opin. Struct. Biol. 4,* 574−581.

Davis, J. H. (1983) *Biochim. Biophys. Acta 737,* 117−171.

Davis, J. H. (1993) in *Cholesterol in membrane models* (Finegold, L., Ed.) CRC Press, Boca Raton, FL.

Davis, P. J., & Keough, K. M. W. (1985) *Biophys. J. 48,* 915−918.

Demel, R. A., & de Kruijff, B. (1976) *Biochim. Biophys. Acta 457*, 109−131.
Earp, H. S., Dawson, T. L., Li, X., & Yu, H. (1995) *Breast Cancer Res. Treat. 35*, 115−132.
Fantl, W. J., Johnson, D. E., & Williams, L. T. (1993) *Annu. Rev. Biochem. 62*, 453−481.
Garnier, N., Genest, D., & Genest, M. (1996) *Biophys. Chem. 58*, 225−237.
Grant, C. W. M. (1986) *Chem. Phys. Lipids 40*, 285−302.
Grant, C. W. M., & McConnell, H. M. (1974) *Proc. Natl. Acad. Sci. U.S.A. 71*, 4653−4657.
Grasberger, B., Minton, A. P., DeLisi, C., & Metzger, H. (1986) *Proc. Natl. Acad. Sci. U.S.A. 83*, 6258−6262.
Gullick, W. J., Bottomley, A. C., Lofts, F. J., Doak, D. G., Mulvey, D., Newman, R., Crumpton, M. J., Sternberg, M. J. E., & Campbell, I. D. (1992) *EMBO J. 11*, 43−48.
Haberkorn, R. A., Griffin, R. G., Meadows, M., & Oldfield, E. (1977) *J. Am. Chem. Soc. 99*, 7353−7355.
Hamilton, K. S., Briere, K., Jarrell, H. C., & Grant, C. W. M. (1994) *Biochim. Biophys. Acta 1190*, 367−375.
Hazan, R., Krushel, L., & Crossin, K. L. (1995) *J. Cell. Physiol. 162*, 74−85.
Heldin, C.-H. (1995) *Cell 80*, 213−223.
Henry, G. D., & Sykes, B. D. (1994) *Methods Enzymol. 239*, 525−535.
Hollenberg, M. D. (1991) *FASEB J. 5*, 178−186.
Huang, T. H., Skarjune, R. P., Wittebort, R. J., Griffin, R. G., & Oldfield, E. (1980) *J. Am. Chem. Soc. 102*, 7377−7379.
Hunter, T., Ling, N., & Cooper, J. A. (1984) *Nature 314*, 480−483.
Hynes, N. E., & Stern, D. F. (1994) *Biochim. Biophys. Acta 1198*, 165−184.
Jans, D. A., Peters, R., Zsigo, J., & Fahrenholz, F. (1989) *EMBO J. 8*, 2481−2488.
Keough, K. M. W., Griffin, B., & Matthews, P. L. J. (1989) *Biochim. Biophys. Acta 983*, 51−55.
Killian, J. A., Salemink, I., dePlanque, M. R. R., Lindblom, G., Koeppe, R. E., II, & Greathouse, D. V. (1996) *Biochemistry 35*, 1037−1045.
Lee, K.-C., & Cross, T. A. (1994) *Biophys. J. 66*, 1380−1387.
Lee, K.-C., Huo, S., & Cross, T. A. (1995) *Biochemistry 34*, 857−867.
Lemmon, M. A., & Engelman, D. M. (1994) *Q. Rev. Biophys. 27*, 157−218.
Li, S.-C., & Deber, C. M. (1993) *J. Biol. Chem. 268*, 22975−22978.
MacDonald, P. M., & Seelig, J. (1988) *Biochemistry 27*, 2357−2364.
Marchesi, V. T. (1986) *Adv. Exp. Med. Biol. 205*, 107−120.
McMullen, T. P. W., & McElhaney, R. N. (1995) *Biochim. Biophys. Acta 1234*, 90−98.
Meier, P., Ohmes, E., & Kothe, G. (1986) *J. Chem. Phys. 85*, 3598−3617.
Morrow, M. R., Singh, D. M., & Grant, C. W. M. (1995) *Biophys. J. 69*, 955−964.
Mouritsen, O. G., & Bloom, M. (1993) *Annu. Rev. Biophys. Biomol. Struct. 22*, 145−171.
Mueller, L., Frey, M. H., Rockwell, A. L., Gierasch, L. M., & Opella, S. J. (1986) *Biochemistry 25*, 557−561.
Mühlebach, T., & Cherry, R. J. (1982) *Biochemistry 21*, 4225−4248.
Needham, D., McIntosh, T. J., & Evans, E. (1988) *Biochemistry 27*, 4668−4673.
Nezil, F. A., & Bloom, M. (1992) *Biophys. J. 61*, 1176−1183.
Northwood, I., & Davis, R. J. (1988) *J. Biol. Chem. 263*, 7450−7453.
Oldfield, E., & Chapman, D. (1972) *FEBS Lett. 23*, 285−297.
Oldfield, E., & Meadows, M., Rice, D., & Jacobs, R. (1978) *Biochemistry 17*, 2727−2740.
Opella, S. J. (1986) *Methods Enzymol. 131*, 327−361.
Opella, S. J., & Stewart, P. L. (1989) *Methods Enzymol. 176*, 242−275.
Opella, S. J., Kim, Y., & McDonnell, P. (1994) *Methods Enzymol. 239*, 536−560.
Owicki, J. C., Springate, M. W., & McConnell, H. M. (1978) *Proc. Natl. Acad. Sci. U.S.A. 75*, 1616−1619.
Pinto da Silva, P. (1987) in *EM of Proteins*, Vol 6, *Membranous Structures* (Harris, J. R., & Horne, R. W., Eds.) pp 1−38, Academic Press, London.
Prosser, R. S., Daleman, S. I., & Davis, J. H. (1994) *Biophys. J. 66*, 1415−1428.
Ramachandran, G. N., & Sasisekharan, V. (1968) *Adv. Protein Chem. 23*, 283−437.
Renou, J. P., Giziewicz, J. B., Smith, I. C. P., & Jarrell, H. C. (1989) *Biochemistry 28*, 1804−1814.
Rigby, A. C., Barber, K. R., Shaw, G. S., & Grant, C. W. M. (1996) *Biochemistry 35*, 12591−12601.
Rost, B. (1996) *Methods Enzymol. 266*, 525−539.
Schlessinger, J. (1988) *Biochemistry 27*, 3119−3123.
Seelig, J. (1977) *Q. Rev. Biophys. 10*, 353−418.
Segrest, J. P., Gulik-Krzywicki, T., & Sardet, C. (1974) *Proc. Natl. Acad. Sci. U.S.A. 71*, 3294−3298.
Siminovitch, D. J., Ruocco, M. J., Olejniczak, E. T., Das Gupta, S. K., & Griffin, R. G. (1988) *Biophys. J. 54*, 373−381.
Smith, I. C. P. (1984) *Biomembranes 12*, 133−168.
Smith, S. O., & Peersen, O. B. (1992) *Annu. Rev. Biophys. Biomol. Struct. 21*, 25−47.
Smith, S. O., & Bormann, B. J. (1995) *Proc. Natl. Acad. Sci. U.S.A. 92*, 488−491.
Smith, S. O., Jonas, R., Braiman, M., & Bormann, B. J. (1994) *Biochemistry 33*, 6334−6341.
Smith, S. O., Smith, C. S., & Bormann, B. J. (1996) *Nat. Struct. Biol. 3*, 252−258.
Sternberg, M. J. E., & Gullick, W. J. (1990) *Protein Eng. 3*, 245−248.
Thewalt, J. L., & Bloom, M. (1992) *Biophys. J. 63*, 1176−1181.
van der Geer, P., & Hunter, T. (1994) *Annu. Rev. Cell Biol. 10*, 251−337.
Weisz, K., Gröbner, G., Mayer, C., Stohrer, J., & Kothe, G. (1992) *Biochemistry 31*, 1100−1112.
Wofsy, C., Goldstein, B., Lund, K., & Wiley, H. S. (1992) *Biophys. J. 63*, 98−110.
Yamanaka, N., & Deamer, D. W. (1976) *Biochim. Biophys. Acta 426*, 132−147.
Yarden, Y., & Ullrich, A. (1988) *Annu. Rev. Biochem. 57*, 443−478.
Yeagle, P. L. (1985) *Biochim. Biophys. Acta 822*, 267−287.

BI970547Z